

# Targeting chemical carcinogenesis: $\alpha$ -pinene and $\beta$ -limonene as chemopreventive agents against NNK/TCDD- and urethane-induced lung tumorigenesis

Kuo-Ching Huang <sup>a,b,1</sup>, Vui-Hyen Chew <sup>a,1</sup>, Yu-ying Chen <sup>a,1</sup>, Huey-Jen Su <sup>a</sup>,  
Hao-Ting Chang <sup>c</sup>, Rong-Jane Chen <sup>d,\*</sup>, Ying-Jan Wang <sup>a,\*\*</sup>

<sup>a</sup> Department of Environmental and Occupational Health, College of Medicine, National Cheng Kung University, 138 Sheng-Li Road, Tainan 70428, Taiwan

<sup>b</sup> Division of Nephrology, Department of Internal Medicine, Chi Mei Hospital, Liouying, No.201, Liouying Dist., Tainan City 73657, Taiwan

<sup>c</sup> Department of Geomatics, College of Engineering, National Cheng Kung University, Tainan, Taiwan

<sup>d</sup> Department of Food Safety/Hygiene and Risk Management, College of Medicine, National Cheng Kung University, Tainan 70428, Taiwan

## Abstract

Lung cancer is the leading cause of cancer-related deaths worldwide, driven by carcinogens such as tobacco-derived nitrosamines, dioxins, and urethane. This study evaluated the chemopreventive effects of two monoterpenes,  $\alpha$ -pinene and  $\beta$ -limonene, using NNK/TCDD- and urethane-induced lung tumor models and A549 lung cancer cells. Both compounds significantly reduce tumor number and size, with enhanced effects when combined. Mechanistic studies revealed suppression of PRC1,  $\beta$ -catenin, and c-Myc, alongside activation of p53, Bax, and caspase-3, indicating inhibition of the PRC1–Wnt/ $\beta$ -catenin pathway and induction of apoptosis. These findings suggest  $\alpha$ -pinene and  $\beta$ -limonene as safe, promising agents for lung cancer chemoprevention.

**Keywords:** Monoterpenes, NNK, PRC1–Wnt– $\beta$ -catenin, TCDD, Urethane

## 1. Introduction

Since the 1950s, lung cancer has consistently represented the leading cause of cancer-related mortality globally, underscoring its substantial impact on public health [1,2]. Non-small cell lung cancer (NSCLC), accounting for approximately 85% of all lung cancer cases, has been historically associated with poor prognosis, primarily due to late-stage diagnosis and limited efficacy of conventional therapeutic interventions [3]. Although chemoradiotherapy and targeted therapy has advanced considerably, disease progression remains largely unavoidable in patients with advanced NSCLC, highlighting the urgent need for

improved therapeutic and preventive strategies [4]. Environmental exposures are critical determinants of lung cancer susceptibility, where respirable and food-borne contaminants serve as major etiological agents, influencing key cellular signaling networks that regulate gene expression, DNA repair fidelity, hormonal regulation, and inflammatory responses [4,5]. Chemical carcinogenesis is a multistage process wherein xenobiotics or their reactive metabolites induce irreversible alterations in cellular homeostasis, driving aberrant cell proliferation and malignant transformation [6]. Cancer prevention is widely regarded as a key strategy for reducing the overall healthcare burden and improving public health outcomes [7–9].

Received 22 September 2025; accepted 17 November 2025.

Available online 15 December 2025

\* Corresponding author at: Department of Food Safety/Hygiene and Risk Management, College of Medicine, National Cheng Kung University, Tainan 70428, Taiwan.

\*\* Corresponding author at: Department of Environmental and Occupational Health, College of Medicine, National Cheng Kung University, 138 Sheng-Li Road, Tainan 70428, Taiwan.

E-mail addresses: [z10808035@email.ncku.edu.tw](mailto:z10808035@email.ncku.edu.tw) (R-J Chen), [yjwang@mail.ncku.edu.tw](mailto:yjwang@mail.ncku.edu.tw) (Y-J Wang).

<sup>1</sup> Kuo-Ching Huang, Vui-Hyen Chew, and Yu-ying Chen contributed equally to this work.

Cancer chemoprevention involves using natural, synthetic, or biological agents to prevent or reverse cancer development. Research now focuses on natural compounds with low toxicity and multi-target effects, offering a safer, more effective approach. Their ability to modulate multiple pathways makes them promising candidates for addressing cancer's complexity and advancing preventive strategies [10,11]. Terpenes, a structurally diverse class of plant-derived secondary metabolites, have garnered significant interest as potential anticancer agents due to their capacity to suppress tumor growth and induce apoptosis in malignant cells [12]. The anticancer effects induced by terpenes have been reported in several pathways. One of the most prominent biological properties of terpenes is their anti-inflammatory activity. Many terpenes regulate immune responses and alleviate inflammation by suppressing key enzymes and signaling pathways involved in the inflammatory process. Additionally, certain terpenes exhibit antioxidant properties, helping to protect cells from damage induced by free radicals and oxidative stress [12]. Terpenes also exert cytotoxic effects by intrinsically inducing apoptosis, primarily through oxidative stress resulting from elevated ROS levels. In addition, monoterpenes exhibit cytostatic properties by causing cell cycle arrest and suppressing cell invasion and migration [13]. Preclinical studies have consistently demonstrated the efficacy of various terpenes against a wide range of tumor types [14]. Among the most extensively studied monoterpenes,  $\alpha$ -pinene and  $\beta$ -limonene, abundant constituents of essential oils, exhibit favorable pharmacokinetic profiles, including low toxicity and high bioavailability, supporting their potential use as alternatives in cancer chemoprevention and therapy [15].

The tumorigenesis animal model effectively simulates tumor development and malignant transformation mechanisms while enabling the evaluation of diverse therapies and preventive strategies, making it an essential tool in cancer research [16]. For example, 4-(Methylnitrosamino)-1-(3-pyridyl)-1-butanone (NNK), a tobacco-specific nitrosamine present in cigarette smoke, inducing lung adenomas and adenocarcinomas in A/J mice [17]. 2,3,7,8-Tetrachlorodibenzo-p-dioxin (TCDD), a ubiquitous environmental contaminant, is recognized as a multisite, multispecies carcinogen with prominent tumor-promoting activity. Experimental evidence demonstrates that TCDD significantly enhances tumor development in various organs, including the lungs of mice [18–20]. In addition, urethane (ethyl carbamate), a fermentation

by-product commonly detected in alcoholic beverages and fermented foods, was identified as a potent lung carcinogen capable of inducing tumors in 100% of susceptible mouse strains [21]. Metabolism study showed that approximately 90% of urethane is hydrolyzed to ethanol, ammonia and carbon dioxide by liver microsomal esterases (carboxylesterases), with only 5% of urethane excreted as unchanged. Urethane is transformed by cytochrome P450 enzyme CYP2E1 to vinyl carbamate, resulting in epoxide formation (vinyl carbamate epoxide), which covalently binds to DNA and can result in base misincorporation during DNA replication, leading to point mutations [22]. Urethane undergoes metabolic activation to form electrophilic intermediates that generate DNA adducts and initiate molecular events involving dysregulated cell proliferation, inflammation, ultimately leading to the development of lung adenomas and adenocarcinomas [23]. This study will employ two chemically induced tumorigenesis animal models to simulate environmental exposures and evaluate the potential combined effects of different carcinogenic mechanisms.

Regarding the underlying mechanisms, polycomb repressive complex 1 (PRC1) plays a critical role in lung tumorigenesis by epigenetically silencing tumor suppressor genes. PRC1 components are frequently upregulated in lung cancer and promote uncontrolled proliferation and resistance to therapy [24]. PRC1 enhances Wnt/ $\beta$ -catenin signaling by repressing Wnt pathway inhibitors and inhibiting GSK3 $\beta$  activity, which prevents  $\beta$ -catenin degradation [25,26]. Accumulated nuclear  $\beta$ -catenin activates downstream targets such as c-Myc, a potent oncogene involved in cell cycle progression, metabolic reprogramming, and maintenance of cancer stemness. The PRC1–Wnt/GSK3 $\beta$ –c-Myc signaling axis represents a central mechanism by which PRC1 drives lung cancer initiation, progression, and malignancy [25,27]. In addition, apoptosis is a tightly regulated process that eliminates damaged or abnormal cells, and its dysregulation is central to lung tumorigenesis. Suppression of key apoptotic mediators, such as caspase-3, Bcl-2 family proteins, and p53, allows malignant cells to evade programmed cell death and accumulate genetic mutations [28,29]. Caspase-3, a crucial executioner caspase, is often downregulated or inactivated in lung cancer, contributing to tumor survival, therapy resistance, and disease progression [30].

In our earlier studies, we established a two-stage lung tumorigenesis model by administering a single low dose of NNK combined with TCDD to A/J mice [18,31]. We also established a urethane-

induced murine lung tumorigenesis model and found that pterostilbene, a natural phytoalexin, exerts chemopreventive effects by inhibiting EGFR and its downstream signaling pathways, thereby delaying cell cycle progression and promoting apoptosis [32]. The goal of our current study was, therefore, to examine the effects of  $\alpha$ -pinene and  $\beta$ -limonene on lung cancer and to explore their mechanisms of action. To accomplish these goals, we employed NNK/TCDD- and urethane-induced lung tumorigenesis models in mice treated with  $\alpha$ -pinene and  $\beta$ -limonene. We investigated the effects of  $\alpha$ -pinene and/or  $\beta$ -limonene on tumor burden, the PRC1–Wnt/ $\beta$ -catenin signaling axis, and the apoptosis pathway, including p53, Bcl-2/Bax, and caspase-3, in animal models, and further confirmed the findings in the A549 lung cancer cell model.

## 2. Materials and methods

### 2.1. In vivo lung carcinogenic model

#### 2.1.1. NNK/TCDD-induced lung carcinogenic model

NNK/TCDD-induced *in vivo* lung cancer model was followed by previous study [31]. Each group of three female A/J mice (6–8 weeks old) were randomly divided into 10 different groups. Low or high dose NNK (10 or 20 mg/mL/mouse) were given intraperitoneally on week one of the experiment (Group 2 to 10). On week two, 5  $\mu$ g/kg b.w. of TCDD was given as a loading dose and a subsequent maintenance dose of 1.42  $\mu$ g/kg b.w. TCDD was given once a week for an additional 3 weeks (Group 7 to 10). 10 mg/kg b.w.  $\alpha$ -pinene or  $\beta$ -limonene were orally fed thrice per week throughout the study. They were given a week prior NNK injection in Group 3–5 to assess the chemopreventive ability of the dietary monoterpenes upon carcinogen exposure. However, for Group 8–10  $\alpha$ -pinene and  $\beta$ -limonene were given a week after NNK administration to assess their suppressing ability in lung tumor promotion and progression. The mice were humanely euthanized after 30 weeks of study. Blood samples and lung tissues were collected for subsequent observation. All animal experiments followed the guidelines of the animal center institute and were approved by the Institutional Animal Care and Use Committee of National Cheng Kung University, Taiwan (Approval No.: 109226).

#### 2.1.2. Urethane-induced lung carcinogenic model

The protocol of urethane induced lung cancer model was modified from previous study [33]. Each group of three female ICR mice (6–8 weeks old)

were interperitoneally injected with urethane (600 mg/kg b.w.; dissolved in saline) weekly for eight consecutive weeks. All mice were housed in pathogen-free environments, individual ventilated cages with a 12-h duration of light/dark. All mice were fed with normal diet and water ad libitum. Mice first received an injection of urethane, then different dose of  $\alpha$ -pinene or  $\beta$ -limonene (40 mg/kg b.w. and 200 mg/kg b.w.; dissolved in corn oil) were given thrice a week via intragastric administration for 12 weeks. 13 weeks after the first urethane injection, the mice were humanely euthanized. Blood and organ samples were collected for further analysis. All animal experiments followed the guidelines of the animal center institute and were approved by the Institutional Animal Care and Use Committee of National Cheng Kung University, Taiwan (Approval No.: 109226).

### 2.2. Serum biochemistry analysis and hematoxylin & eosin staining

Blood samples were collected into tube without anticoagulant and placed in room temperature for 30 min before submitted to a 4 °C, 2500 rpm centrifuge. The supernatant (blood serum) was then collected and stored in –80 °C until further use. Level of GPT (U/L), GOT (U/L), BUN (mg/dL), CRE (mg/dL), and ALB (g/dL) of each group were analyzed with Fuji Dri-Chem 3500i chemistry analyzer (Fuji, JP).

For hematoxylin & eosin staining, tissues were first fixed in 3.7% neutral buffered formaldehyde after sacrificed, samples were then dehydrated and paraffin-embedded for further histopathological analysis. For histological analysis, the tissue sections were stained with hematoxylin and eosin followed by previous protocol [34]. Tumor diameters were measured by ImageJ software, and the tumor burden of each group were calculated.

### 2.3. Immunohistochemistry staining

Paraffin-embedded slides were deparaffinized and rehydrated with alcohol gradient and washed with 1x PBS twice to remove unnecessary residue. The hydrated tissue sections were boiled with citrate buffer (pH 6.0) for 15 min for antigen removal before treating with 3% hydrogen peroxide. IHC Select® Immunoperoxidase Secondary Detection System (Millipore, USA) was used to perform immunohistochemical staining. Briefly, tissue sections were blocked with blocking reagent for 5 min at room temperature, then incubated with aliquots of antibodies against anti-PRC1, anti-cleaved-

caspase-3, anti- $\beta$ -catenin, anti-GSK-3 $\beta$ , and anti-c-myc (Abcam, UK) for an hour. After washing, aliquots of biotinylated secondary antibodies were added. Color development was performed using streptavidin HRP and DAB chromogen. Finally, the slides were counterstained using hematoxylin and examined under light microscopy. Three views were randomly chosen for each treatment group, and the positive stained area was used to quantify protein expression. The intensity of protein expression was quantified by using TissueFAX microscope (TissueGnostics GmbH, Austria).

#### 2.4. *In vitro* study

Human lung epithelial carcinoma cell line A549 (BCRC 60074) was cultured in DMEM (Gibco, NY, USA) supplemented with 10% fetal bovine serum (Gibco, NY, USA) and antibiotics containing 10,000 U/mL penicillin as well as 10,000  $\mu$ g/mL streptomycin at 37 °C in a 5% CO<sub>2</sub> atmosphere.

#### 2.5. Cell viability assay

Cells were collected according to the cell culture procedure. Cells were plated in 96-well plates at a density of 10,000 cells. After overnight growth, the medium was replaced with 100  $\mu$ L containing different doses of alpha-pinene or D-limonene. After incubation, the medium was removed and added MTT solution (10x-diluted from a 5 mg/mL stock solution) into each well. After 1-h incubation, the formazan was dissolved in DMSO. optical density (OD) of 570 nm was measured in ELISA reader (SpectraMax 340PC384, Molecular Devices).

#### 2.6. Apoptosis assay

Apoptosis assay of the treated cells was performed with an Annexin V/PI detection kit (BD Pharmingen, 556547), according to the manufacturer procedure. In short, both cell medium and trypsinized cells were collected to a 15 mL tube prior before submitted to 3-min centrifugation. After discarding the supernatant, the cells were resuspended with 1x PBS and centrifuged for the second time. The supernatant was then replaced with 500  $\mu$ L binding buffer. After resuspension, transfer 100  $\mu$ L of cell solution to a FASC tube. 2.5  $\mu$ L of Annexin V and PI were added to the tubes, which were then being kept in dark environment for 30 min. The apoptotic rate of cancer cells was then measured and analyzed with a flow cytometer (CytoFLEX, BD, USA).

#### 2.7. Western blot analysis

For Western blotting, cell or tissue extracts were prepared by homogenizing in lysis buffer. Protein concentration was determined using a BCA assay, and approximately 10  $\mu$ g of protein was mixed with Laemmli buffer and boiled. Whole-protein extracts were then separated on 6–15% SDS-polyacrylamide gels and transferred onto polyvinylidene difluoride (PVDF) membranes (Merck Millipore, Darmstadt, Germany). After blocking for 1 h, the membranes were incubated with primary antibodies at a 1:1000 dilution. The antibodies of anti-PRC1, anti-caspase-3, anti- $\beta$ -catenin, anti-GSK-3 $\beta$ , and anti-c-myc were purchased from Cell Signaling (Beverly, MA, USA). After hybridization, the membrane was washed with 1  $\times$  TBST and then incubated with HRP-conjugated anti-mouse (Bio-Legend, San Diego, CA, USA) or anti-rabbit secondary antibodies (Jackson ImmunoResearch Lab Inc., West Grove, PA, USA) at a 1:10,000 dilution. Immunoreactive proteins were detected using the Immobilon Western chemiluminescence HRP substrate and visualized with the iBright imaging system (Thermo Fisher, USA).

#### 2.8. Statistical analysis

All data were presented with the mean  $\pm$  SD of at least three independent experiments. Student's t-test and one-way analysis of variance were used for data analysis. P < 0.05 was considered indicative of statistical significance.

### 3. Results

#### 3.1. Antitumor effects of $\alpha$ -pinene and D-limonene in NNK/TCDD-induced lung carcinogenic model

To understand the antitumor efficacy of  $\alpha$ -pinene and D-limonene in lung cancer, we utilized a well-established NNK/TCDD-induced lung cancer model in this study. All A/J mice were in healthy condition throughout the course of 30-week study apart from group NNK(L)+TCDD, which experienced body hair loss during the experiment (Supp. Fig. 1) (<https://doi.org/10.38212/2224-6614.3576>). Tumor incidence and multiplicity are listed in Table 1. Results showed 100% lung tumor incidence in mice treated with NNK(L), NNK(H) and NNK(L)+TCDD. Mice treated with NNK(H) and NNK(L)+TCDD had the highest tumor multiplicity among all groups, with 6.0  $\pm$  1.73 and 6.0  $\pm$  3.16 respectively. The monoterpenes inhibited lung tumorigenesis by suppressing tumor multiplicity upon co-treating

Table 1. Lung tumor incidence and multiplicity of NNK-TCDD exposure model.

Treatment	Tumor bearing mice/Total mice	Tumor incidence (%)	Tumor multiplicity
Control	0/4	0	0
NNK (L)	4/4	100	3.3 ± 0.96
NNK (L)+ $\alpha$ P	4/4	100	3.0 ± 1.83
NNK (L)+dL	4/4	100	3.8 ± 0.50
NNK (L)+C	4/4	100	2.0 ± 0.82
NNK (H)	4/4	100	4.8 ± 2.87
NNK (L)+TCDD	4/4	100	7.0 ± 2.58
NNK (L)+TCDD+ $\alpha$ P	4/4	100	3.0 ± 1.41 <sup>a</sup>
NNK (L)+TCDD+dL	4/4	100	3.7 ± 2.51
NNK (L)+TCDD+C	4/4	100	3.7 ± 2.08

Tumor incidences are calculated as the number of tumor-bearing mice/total mice (%). Tumor multiplicity is the average tumor number on tumor-bearing mice. Data expressed as mean ± standard deviation.

<sup>a</sup>  $p < 0.05$  compared to NNK(L)+TCDD group.

with NNK and TCDD, lung tumor nodules spreading across the surface of lungs that were exposed to NNK and TCDD (Fig. 1B). Lungs appeared darker in lungs that were given NNK(H) as well as NNK+TCDD. In contrast to the carcinogen groups, mice that were fed either individual or combined monoterpenes have lesser number of nodules on their lung surfaces and the lung texture was relatively smoother. All tumors were seen as cuboid cells having hyperchromatic nuclei, which fits the histological feature of adenoma (Fig. 1A). Larger tumors could be seen in mice treated with NNK(L) and NNK(H) whereas numerous small adenomas were presented in lungs of mice exposed to NNK+TCDD (Fig. 1B). Furthermore, there is a decrease in tumor burden in NNK(L)+ $\alpha$ P, NNK (L)+dL, and NNK(L)+ Combined group compared to NNK(L) group alone. Significant reduction of tumor burden was found in NNK(L)-treated mice fed with  $\alpha$ -pinene, d-limonene, and the combined groups, whereas there was no significant difference between the groups of NNK+TCDD-treated mice (Fig. 1C). To further explore the antitumor mechanism of  $\alpha$ -pinene and d-limonene *in vivo*, immunostaining of PRC1,  $\beta$ -catenin, and c-myc expression were conducted and demonstrated decreasing after  $\alpha$ -pinene and d-limonene treatment, while caspase-3 activity was up-regulated. Overall, these data suggested that both  $\alpha$ -pinene and d-limonene inhibited tumor promotion and progression by limiting tumor proliferation and inducing apoptosis in NNK/TCDD-induced lung cancer.

### 3.2. Antitumor effects of $\alpha$ -pinene and d-limonene in urethane-induced lung carcinogenic model

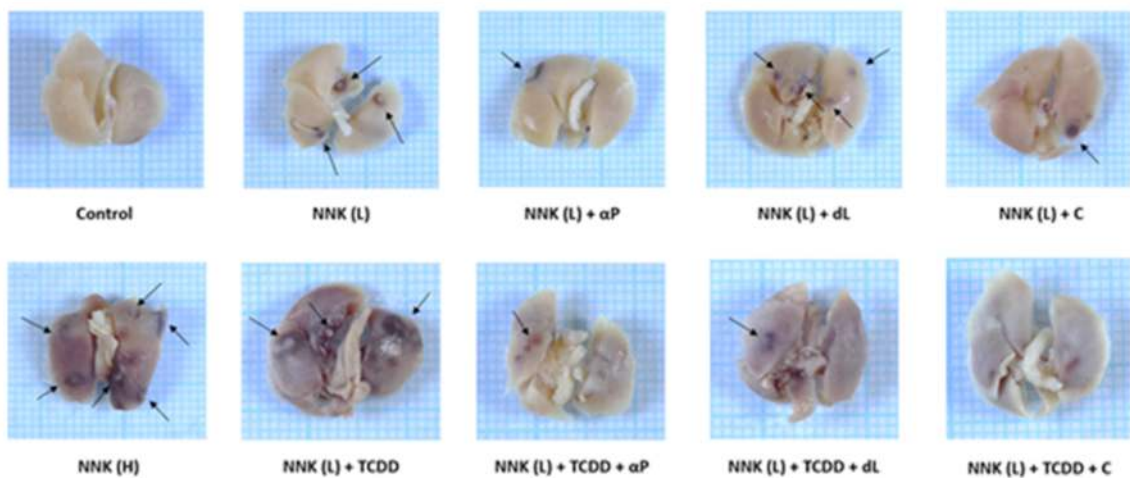
In the urethane-induced lung carcinogenic model, results showed 100% lung tumor incidence in all groups. However, tumor multiplicity

decreased in urethane+ $\alpha$ P, urethane+dL, and urethane+combined group (Table 2). The appearance of the lungs and the diameter of tumor nodules in tissue sections showed that the groups treated with  $\alpha$ -pinene and d-limonene had a certain degree of reduction in both the number and size of tumors compared to the urethane-alone treatment group (Fig. 3A and B), indicating that the intervention of  $\alpha$ -pinene and d-limonene reduced tumor burden to some extent. Significant reduction of tumor burden was found in urethane-treated mice fed with  $\alpha$ -pinene and the combined groups, whereas there was no significant difference with d-limonene groups (Fig. 3C). IHC stain also showed  $\alpha$ -pinene and d-limonene treatment reduced PRC1,  $\beta$ -catenin, and c-myc expression and upregulated caspase-3 expression (Fig. 4A and B). Overall,  $\alpha$ -pinene and d-limonene demonstrated the ability to attenuate tumor development in both lung cancer animal models.

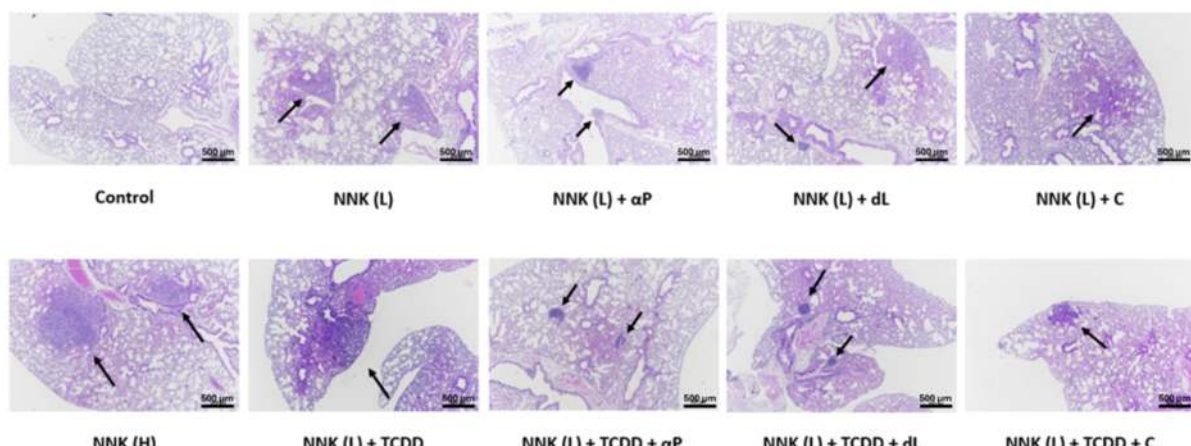
### 3.3. $\alpha$ -pinene and d-limonene exerted apoptosis effect in lung cancer cells through PRC1-wnt/ $\beta$ -catenin signaling

To investigate the antitumor effect of  $\alpha$ -pinene and d-limonene *in vitro*, A549 was used in this study. Cells were treated with various concentration of  $\alpha$ -pinene and/or d-limonene ranging from 0, 0.1, 0.3, 0.5, and 0.7 mM for 24 h. Results showed that both individual and combined monoterpenes inhibited cell growth in A549 cells in a dose-dependent manner compared to the control cells (Fig. 5A). After 24 h treatment of  $\alpha$ -pinene and d-limonene, PI-Annexin V assay showed significant increase of apoptotic cells (Fig. 6A). Expression of Bax and caspase-3 were elevated and the expression of Bcl-2 decreased in  $\alpha$ -pinene- and d-limonene-treated A549 cells (Fig. 6B). Together, these data indicate that  $\alpha$ -pinene and d-limonene affect the process of apoptosis.

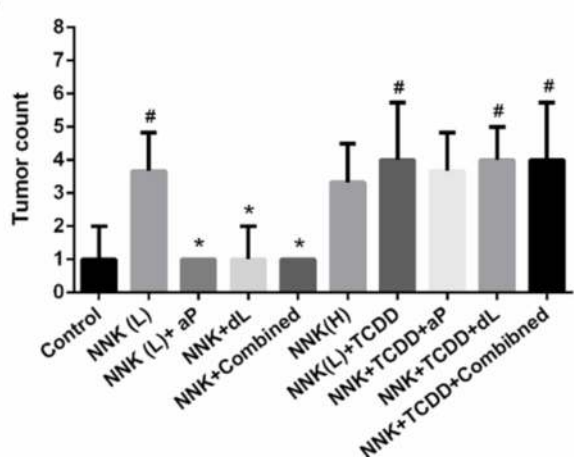
(A)



(B)



(C)



(D)

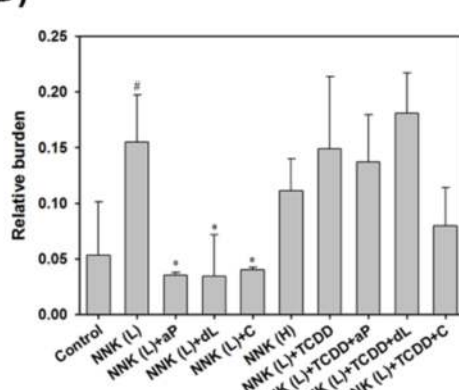


Fig. 1. Preventive Effects of  $\alpha$ -Pinene and *d*-Limonene on NNK/TCDD-induced lung cancer model. (A) Gross appearances of lung tumors on lungs of each group. Black arrow showed lung tumor as whitish nodule in the lung. (B) HE stains on lung sections of each group, black arrow indicates lung tumor as whitish nodule in the lung. Scale bar = 500  $\mu$ m. (C) Number of nodules in each treatment group. (D) Relative lung tumor burden of the mice, which is defined as the average amount of nodules/weight of tumor-bearing mice. All data are presented as the mean  $\pm$  S.D.;  $n = 3$ ;  $\#p < 0.05$  compared to control,  $*p < 0.05$  compared to NNK(L) group.

Table 2. Lung tumor incidence and multiplicity of urethane exposure model.

Treatment	Tumor bearing mice/Total mice	Tumor Incidence (%)	Tumor multiplicity
Control	0/4	0	0
Urethane (U)	4/4	100	19.0 ± 11.27
U+αP (L)	4/4	100	4.5 ± 1.91
U+αP (H)	4/4	100	12.7 ± 3.51
U+dL (L)	4/4	100	10.3 ± 4.73
U+dL (H)	4/4	100	3.7 ± 1.53
U+Combined (L)	4/4	100	6.0 ± 2.65
U+Combined (H)	4/4	100	4.7 ± 0.58

Tumor incidences are calculated as the number of tumor-bearing mice/total mice (%). Tumor multiplicity is the average tumor number on tumor-bearing mice. Data expressed as mean ± standard deviation.

PRC1 as a key part in the activation of the Wnt/β-catenin pathway in lung adenocarcinoma development [25]. Hence, we hypothesized α-pinene and D-limonene might exert antitumor effect by regulating PRC1 and its downstream target protein, inhibiting cell cytokinesis and proliferation. The western blotting results showed that the monoterpenes up-regulated p53 protein level, down-regulated the protein expressions of PRC1 and β-catenin compared to the control group, indicating the inhibition of cell proliferation activity (Fig. 7A). Based on the results obtained from *in vivo* and *in vitro* we speculated that α-pinene and D-limonene down-regulated PRC1 expression, inhibiting activation of APC/β-catenin destruction complex, reducing nuclear translocation of β-catenin (Fig. 8).

#### 4. Discussion

Monoterpenes, a subclass of terpenoids, have attracted considerable attention due to their wide applications in the cosmetic, food, perfumery, and pharmaceutical industries. Their diverse biological properties, including antioxidants, anti-inflammatory, and anticancer effects, have been well documented [35,36]. Among them, α-pinene and D-limonene have been the focus of numerous reviews highlighting their therapeutic potential [15,37–40]. The proposed anticancer mechanisms of monoterpenes include modulation of oxidative stress, suppression of aberrant cell proliferation, induction of cell cycle arrest, and regulation of oncogenic signaling pathways such as PI3K/Akt and MAPK [15,38,41]. However, despite these promising effects, the antitumor potential of α-pinene and D-limonene in lung cancer models remains underexplored. Our study addressed this gap by investigating the chemopreventive efficacy of α-pinene and D-limonene in two murine lung tumorigenesis models induced by NNK/TCDD and urethane. We observed currently that TCDD further exacerbated

NNK-induced lung tumorigenesis, as evidenced by an increased number of gross lesions and nodules on lung surfaces in co-exposed animals (Fig. 1B). Additionally, the lungs of mice treated with high-dose NNK or NNK+TCDD appeared visibly darker, suggesting more severe pulmonary injury. Significant reduction of tumor burden was found in NNK (L)-treated mice fed with α-pinene, D-limonene, and the combined groups. These findings not only validate the potency of our combined carcinogen model but also underscore the need for effective chemopreventive agents capable of counteracting complex carcinogenic mechanisms. We also found a decreased expression of PRC1, β-catenin, and c-myc in mice treated with α-pinene and/or D-limonene, while caspase-3 activity was up-regulated (Fig. 2A and B). The observed protective effects of α-pinene and D-limonene in these models support their further investigation as potential therapeutic candidates for lung cancer prevention and intervention.

In addition to the NNK/TCDD model, we also employed a urethane-induced lung tumorigenesis model in ICR mice, modified based on the protocol established by Yao et al. [42]. Gross pathological examination revealed that urethane induced multiple pulmonary adenomas of varying sizes. Consistent with our findings in the NNK/TCDD model, α-pinene and D-limonene exerted significant antitumor effects in the urethane model. Notably, co-administration of both monoterpenes resulted in a synergistic reduction in tumor size and number, thereby lowering both overall tumor burden and tumor multiplicity across treatment groups (Fig. 3 and Table 2). Immunohistochemical analysis further indicated that α-pinene and D-limonene downregulated PRC1 expression, leading to suppression of the PRC1/β-catenin signaling axis in lung tissues (Fig. 5). These findings support the therapeutic potential of monoterpenes in chemoprevention, particularly through modulation of PRC1-mediated oncogenic pathways.

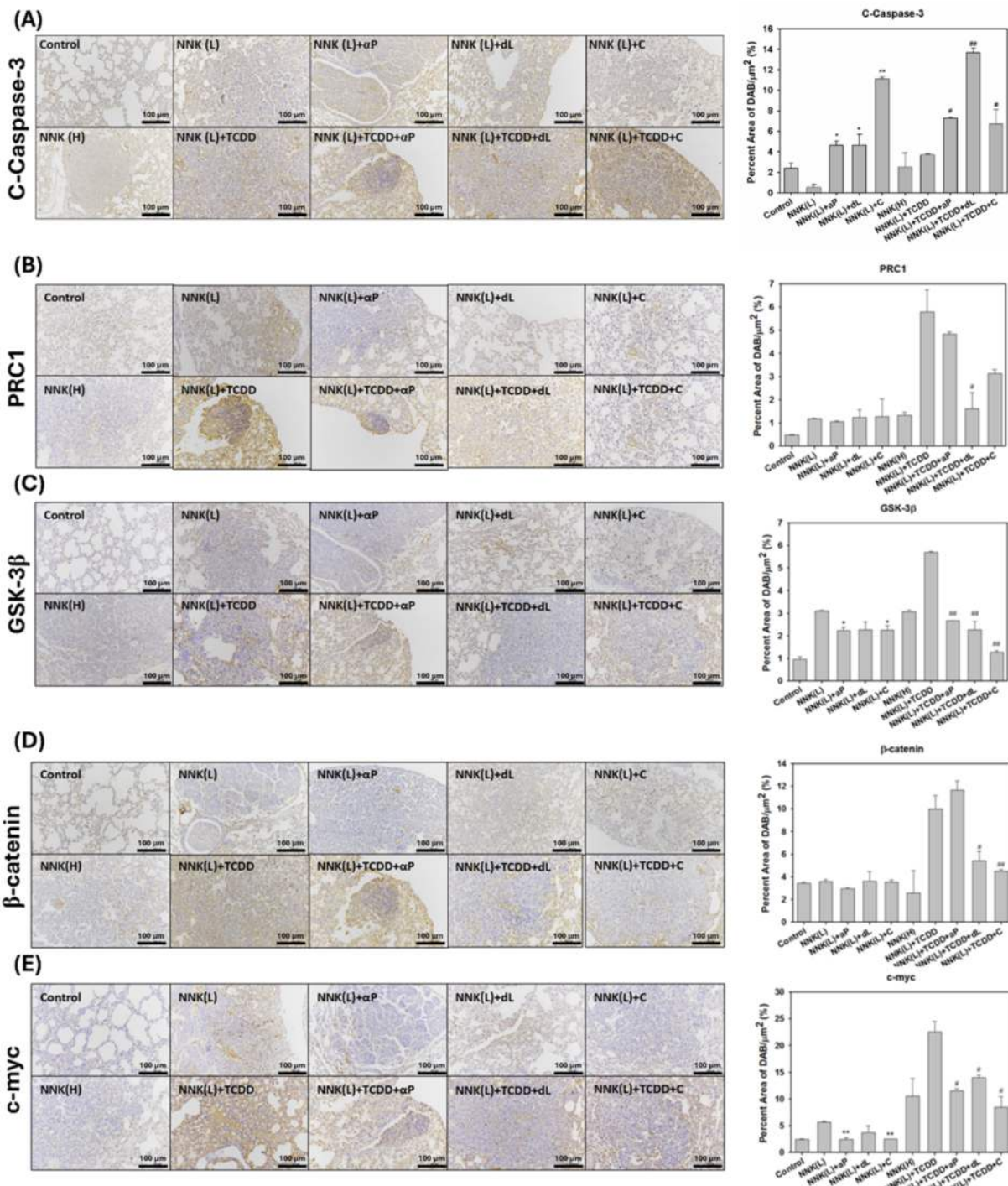
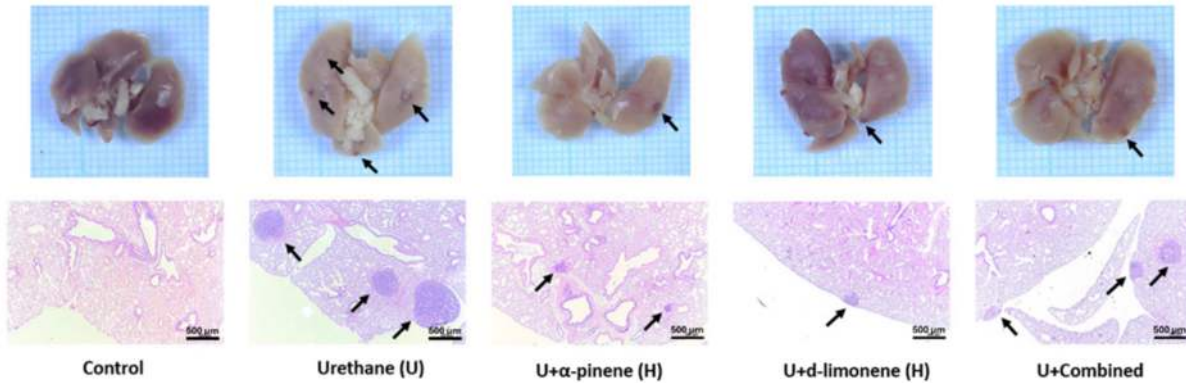


Fig. 2. Effect of  $\alpha$ -pinene and  $d$ -limonene on PRC1-wnt pathway in NNK/TCDD-induced lung cancer model. (A–E) cleaved-Caspase-3, PRC1, GSK-3 $\beta$ ,  $\beta$ -catenin, and c-myc expression performed via immunohistochemical staining. Scale bar = 100  $\mu$ m. Histograms represent the quantification of Caspase-3, PRC1, GSK-3 $\beta$ ,  $\beta$ -catenin, and c-myc expressions. Values were expressed as mean  $\pm$  standard deviation of three mice per group. All data are presented as the mean  $\pm$  S.D.;  $n = 3$ ; \* $p < 0.05$ , \*\* $p < 0.01$  compared to NNK(L) group, # $p < 0.05$ , ## $p < 0.01$  compared to NNK(L)+TCDD group.

(A)



Control

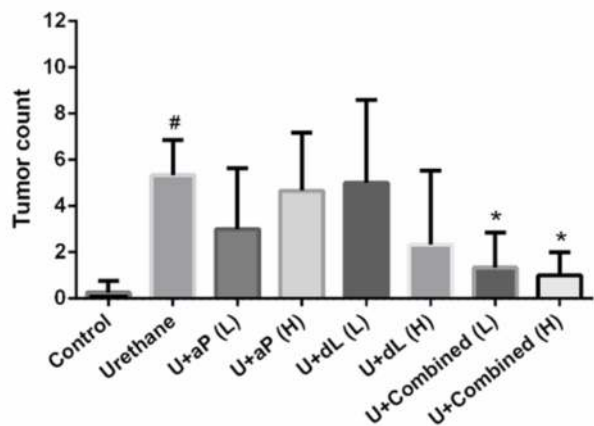
Urethane (U)

U+ $\alpha$ -pinene (H)

U+d-limonene (H)

U+Combined

(B)



(C)

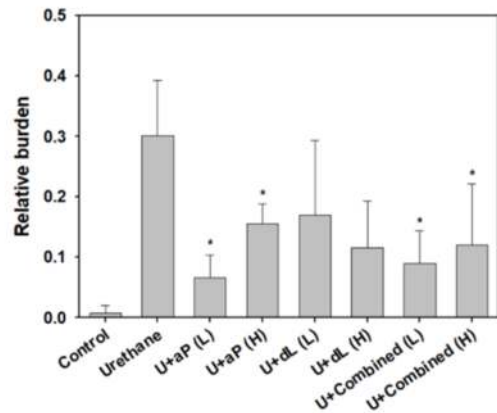


**Fig. 3. Preventive Effects of  $\alpha$ -Pinene and  $d$ -Limonene on Urethane-Induced Lung Tumorigenesis model.** (A) Gross appearances of lung tumors on lungs of each group. Black arrow showed lung tumor as whitish nodule in the lung. HE stains on lung sections of each group, black arrow indicates lung tumor as whitish nodule in the lung. Scale bar = 500  $\mu$ m. (B) Number of nodules in each treatment group. (C) Relative lung tumor burden of the mice, which is defined as the average amount of nodules/weight of tumor-bearing mice. All data are presented as the mean  $\pm$  S.D.;  $n = 3$ ; # $p < 0.05$  compared to control. \* $p < 0.05$  compared to urethane group.

Unexpectedly, mice treated with NNK+TCDD exhibited transient alopecia during the period of the experiment. Hair loss initially appeared as small patches on the dorsal or facial regions and progressively expanded into large, diffuse areas of baldness (Supplement Fig. 1) (<https://doi.org/10.38212/2224-6614.3576>). Interestingly, this hair loss was self-limiting, with full regrowth observed within 4–5 months by the end of the experimental period. A similar phenomenon was previously reported by researchers who found that chronic nicotine exposure induced transient alopecia and muscle sarcomas in A/J mice [43]. In contrast, mice co-treated with NNK+TCDD and either  $\alpha$ -pinene ( $\alpha$ P),  $d$ -limonene (dL), or their combination (C)

displayed minimal or no signs of alopecia, suggesting that monoterpene co-administration may alleviate or prevent balding associated with chemical carcinogen exposure in A/J mice. However, further mechanistic studies are needed to elucidate the underlying biological processes contributing to this unexpected observation.

Although  $\alpha$ -pinene and  $d$ -limonene are classified as Generally Recognized as Safe (GRAS) by regulatory authorities and are extensively utilized as additives in the food and cosmetic industries, both compounds have demonstrated dose-dependent toxicological effects under experimental conditions. Specifically,  $d$ -limonene has been associated with contact dermatitis, hepatotoxicity, and reproductive

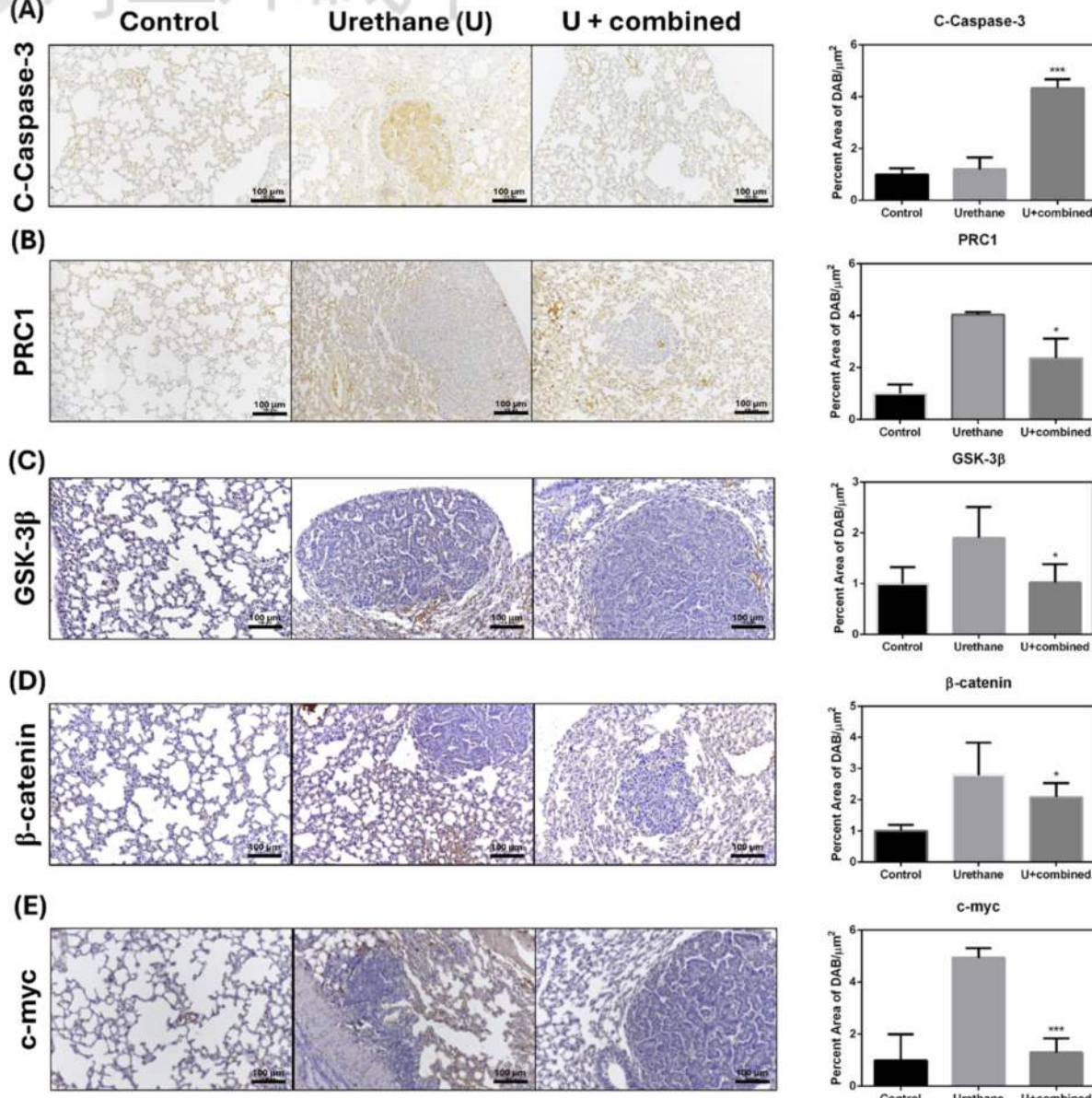
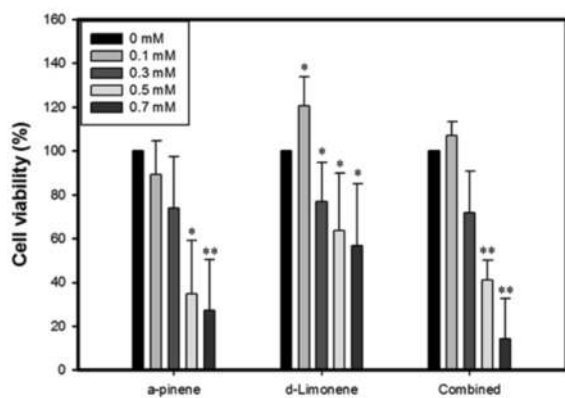


Fig. 4. Effect of  $\alpha$ -pinene and D-limonene on PRC1-wnt pathway in urethane-lung cancer model. Caspase-3, PRC1, GSK-3 $\beta$ ,  $\beta$ -catenin, and c-myc expression performed via immunohistochemical staining. Scale bar = 100  $\mu\text{m}$ . Histograms represent the quantification of cleaved-Caspase-3, PRC1, GSK-3 $\beta$ ,  $\beta$ -catenin, and c-myc expressions. Values were expressed as mean  $\pm$  standard deviation of three mice per group. All data are presented as the mean  $\pm$  S.D.;  $n = 3$ ; \* $p < 0.05$ ; \*\* $p < 0.01$  compared to control, # $p < 0.05$ ; ## $p < 0.01$  compared to urethane group.

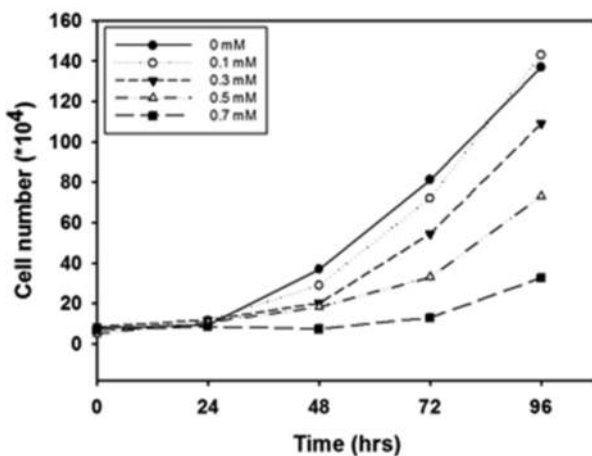
toxicity in animal studies [44]. However, these adverse effects typically occur at supra-physiological doses not reflective of typical human exposure. According to previous risk assessment study of Limonene, human subject exposed to 250 mg/kg/day of Limonene appears to exert no serious adverse effect [45]. In the present study, D-limonene was administered at doses of 40 and 200 mg/kg body weight (bw) three times per week in the urethane-induced lung tumorigenesis model, and at

10 mg/kg bw twice weekly in the NNK/TCDD model. These doses are substantially lower than the established chronic oral No-Observed-Adverse-Effect Level (NOAEL) of approximately 500 mg/kg/day in rodents, as reported by the Flavor and Extract Manufacturers' Association [46] and confirmed by more recent toxicological assessments [47]. Gross pathological examination of the heart, liver, spleen, and kidneys revealed no abnormal morphological changes in either experimental

(A)

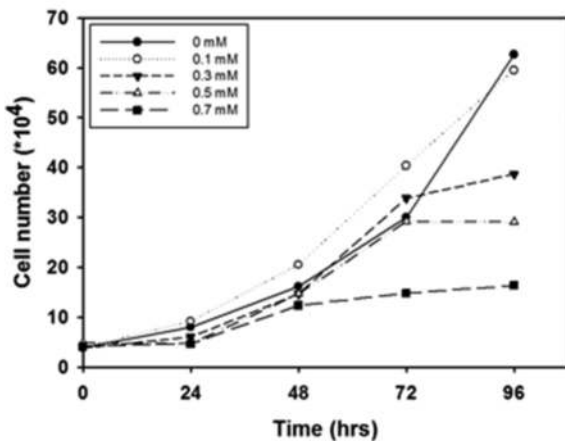


(B)

A549 ( $\alpha$ P)

(C)

A549 (dL)



(D)

A549 (Combined)

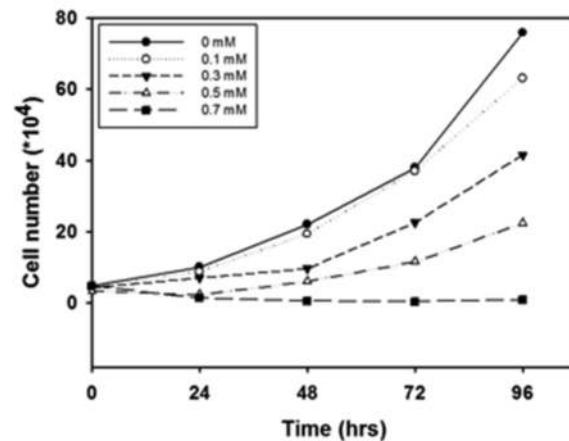


Fig. 5. Antiproliferative effect of  $\alpha$ -pinene and  $\alpha$ -limonene in lung cancer cells. (A) Cell viability of A549 upon treatment of  $\alpha$ -pinene and/or  $\alpha$ -limonene with various concentrations for 24 hr. (B-D) Proliferation rate of A549 upon treatment of  $\alpha$ -pinene and/or  $\alpha$ -limonene with various concentrations and durations. The experiments were performed via Trypan Blue Exclusion assay. Data are expressed as mean  $\pm$  standard deviation from three independent studies. All data are presented as the mean  $\pm$  S.D.;  $n = 3$ ; \*  $p < 0.05$ ; \*\*  $p < 0.01$  compared to control.

model (Supplement Tables 1 and 2) (<https://doi.org/10.38212/2224-6614.3576>). These findings support the safety profile of  $\alpha$ -pinene and  $\alpha$ -limonene and suggest their potential application as chemopreventive agents in lung cancer without inducing significant systemic toxicity.

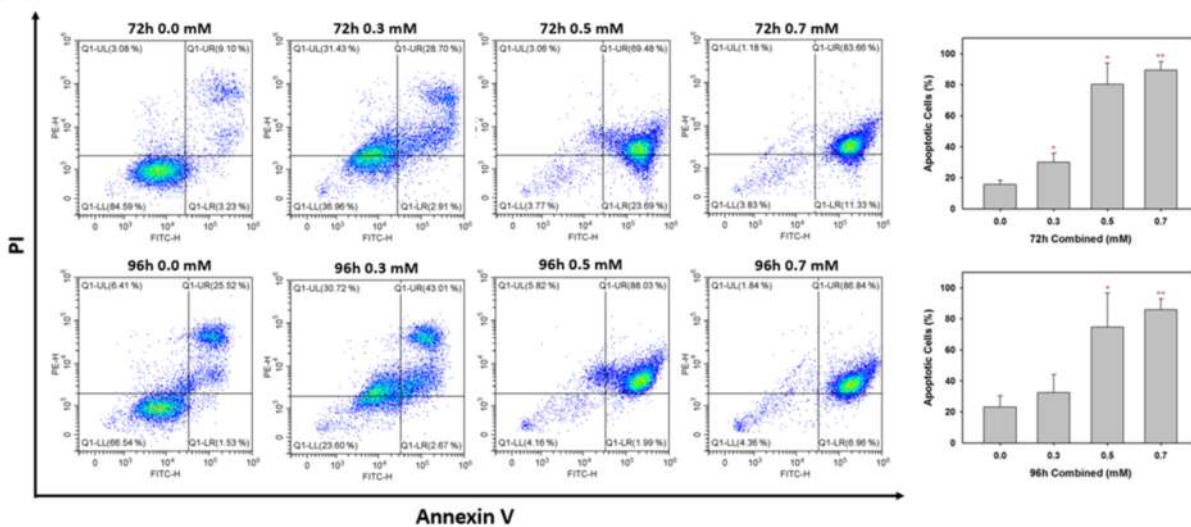
Previous studies have shown the anticancer activity of  $\alpha$ -pinene and  $\alpha$ -limonene. The authors indicated that  $\alpha$ -pinene could suppress hepatoma carcinoma BEL-7402 cells *in vitro* and *in vivo*. Under *in vitro* conditions, BEL-7402 cells were treated with  $\alpha$ -pinene at doses ranging from 0.125 to 8 mg/L, and assessed using MTT method at 24, 48, and 72 h. Mice having BEL-7402 xenograft tumor cells treated with  $\alpha$ -pinene showed significant suppression over 5-FU (fluorouracil) [48].  $\alpha$ -Limonene effects have recently been investigated on T24 human bladder

cancer cells presenting an IC<sub>50</sub> of 9  $\mu$ M. Ye et al. demonstrated that it presented the antitumor capacity to induce cell cycle arrest, suppression of cell migration and invasion, and apoptosis with observation of nuclear fragmentation, chromatin condensation, splitting of the nucleus, increase of Bax and caspase-3, and decrease of Bcl-2 expressions [49], which has similar effects to our current study.

The evasion of programmed cell death is a well-established hallmark of cancer, contributing to tumor progression and resistance to therapy [50]. Apoptosis, a form of programmed cell death, plays a critical role in embryogenesis, tissue development, and homeostasis [51]. Dysregulation of apoptotic pathways has been implicated in the pathogenesis and therapeutic resistance of non-

月旦知識庫

(A)



(B)

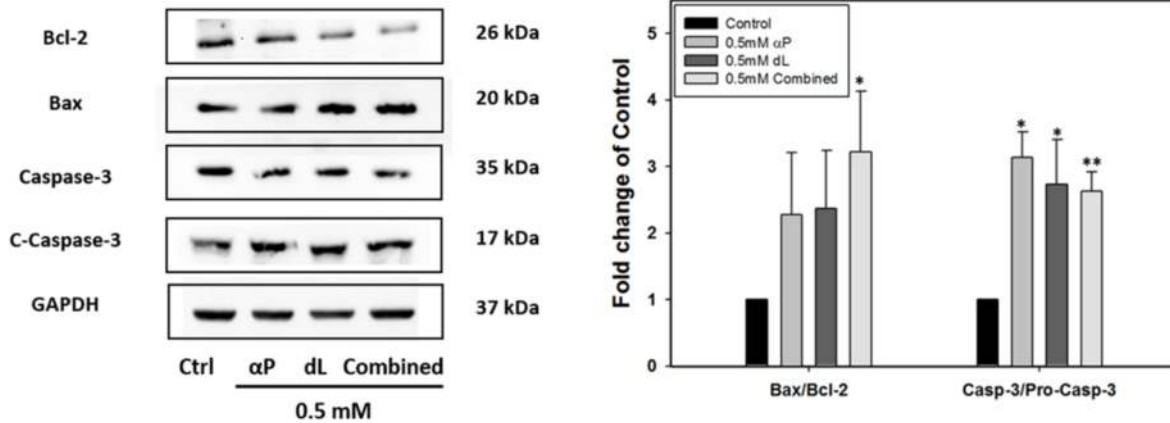
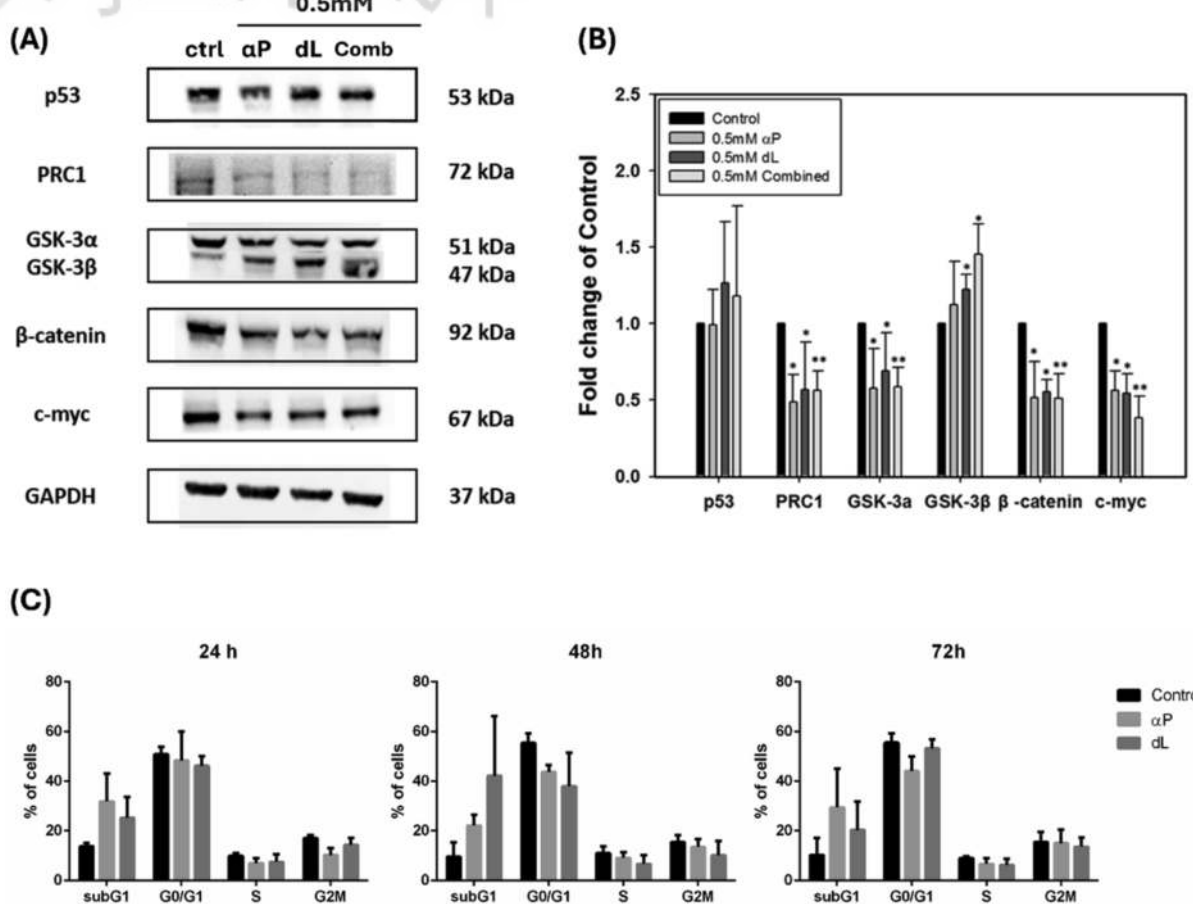


Fig. 6.  $\alpha$ -pinene and  $\alpha$ -limonene Promotion of apoptosis on A549 lung cancer cells. (A) Representative figures of apoptotic cells stained with Annexin V and Propidium Iodide (PI) after treating A549 with combined monoterpenes for 72hr. (B) A549 cells were treated with  $\alpha$ -pinene and/or  $\alpha$ -limonene for 24hr. Apoptosis-related proteins were examined via Western blotting. Protein expressions are quantified using ImageJ software. Data expressed as mean  $\pm$  standard deviation from three independent studies. All data are presented as the mean  $\pm$  S.D.; n = 3; \*p < 0.05; \*\*p < 0.01 compared to control.

small cell lung cancer (NSCLC). Previous studies have reported that  $\alpha$ -pinene and  $\alpha$ -limonene exert pro-apoptotic effects in NSCLC cells [52,53]. In the current study,  $\alpha$ -pinene and  $\alpha$ -limonene treatment significantly enhanced apoptosis in NSCLC tissues, as evidenced by increased caspase-3 expression observed through immunohistochemical analysis (Figs. 3 and 5). Apoptotic progression was further confirmed by flow cytometry using Annexin V staining, which detects phosphatidylserine (PS) externalization on the outer leaflet of the plasma membrane, an early apoptotic marker [54] (Fig. 7A). Additionally, Western blot analysis revealed upregulation of pro-apoptotic proteins Bax and caspase-

3, along with downregulation of the anti-apoptotic protein Bcl-2 in A549 lung cancer cells (Fig. 7B). These findings collectively support the role of  $\alpha$ -pinene and  $\alpha$ -limonene in promoting apoptosis and highlight their potential utility as chemopreventive or therapeutic agents in lung cancer [28–30].

According to a recent multi-factor survival analysis, PRC1 was identified as one of the significantly differentially expressed genes in response to  $\alpha$ -limonene treatment in lung adenocarcinoma (LUAD) [55]. PRC1 plays a critical role in microtubule organization during cytokinesis, and its aberrant overexpression has been observed in lung cancer tissues, where it correlates with poor



**Fig. 7. Regulation of PRC1 and its downstream proteins on A549 lung cancer cells by  $\alpha$ -pinene and d-limonene.** Protein expressions of p53, PRC1, GSK-3 $\alpha$ / $\beta$ ,  $\beta$ -catenin, and c-myc after treated with  $\alpha$ -pinene and/or d-limonene for 24hr were examined via Western blotting. Relative protein expressions are quantified using ImageJ software. Data are expressed as mean  $\pm$  standard deviation from three independent studies. All data are presented as the mean  $\pm$  S.D.;  $n = 3$ ; \*  $p < 0.05$ ; \*\*  $p < 0.01$  compared to control.

prognosis in patients with non-small cell lung cancer (NSCLC) [56]. In addition, Zhan et al. reported a mechanistic link between PRC1 and the Wnt/ $\beta$ -catenin signaling pathway in LUAD, suggesting a broader oncogenic role for PRC1 in lung tumorigenesis [25]. Based on these findings, we hypothesized that  $\alpha$ -pinene and d-limonene may exert chemopreventive effects by inhibiting PRC1 expression and suppressing the activation of its downstream effectors, including GSK3 $\beta$  and c-Myc. Our experimental data support this hypothesis, demonstrating that PRC1 expression is upregulated in lung tumor tissues and that treatment with  $\alpha$ -pinene and d-limonene significantly downregulated both PRC1 and its downstream targets (Figs. 3 and 5). However, it is important to consider that different molecular mechanisms may underlie urethane-induced lung carcinogenesis. Recent studies have identified that urethane-induced pulmonary tumors are frequently driven by oncogenic

mutations at codon Q61 in the Kras gene, which represent a distinct pathway from PRC1-mediated oncogenesis [57,58]. Further studies are warranted to delineate the molecular heterogeneity underlying chemically induced lung tumor models.

## 5. Conclusion

Dietary pollutants such as benzo[a]pyrene from grilled meats, TCDD in fish, and urethane in fermented foods and alcoholic beverages are human carcinogens, with inevitable exposure through diet potentially compounding risks via enhanced effects with other hazardous chemicals. In this study,  $\alpha$ -pinene and d-limonene markedly suppressed lung tumorigenesis *in vivo* and *in vitro* by inhibiting the PRC1/ $\beta$ -catenin/GSK-3 $\beta$  signaling axis and inducing apoptosis, thereby reducing tumor multiplicity in murine lung cancer models. Given that carcinogens like NNK, TCDD, and urethane drive

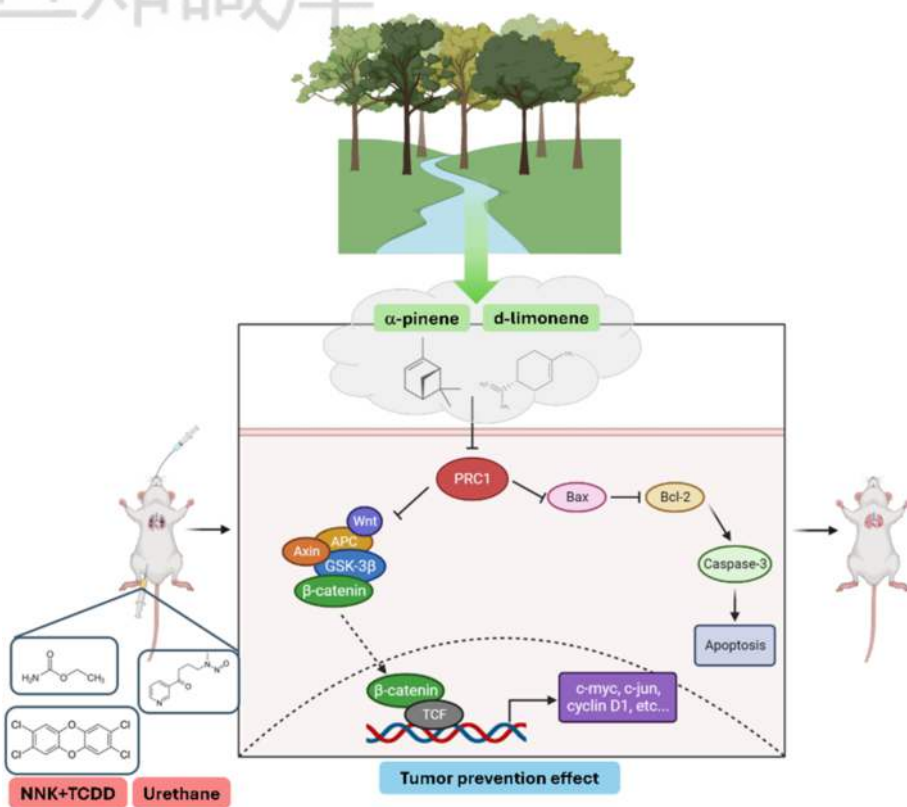


Fig. 8. Treatment with  $\alpha$ -pinene and  $d$ -limonene suppressed lung carcinogenesis by downregulating PRC1, promoting activation of the Wnt/ $\beta$ -catenin signaling pathway, and inducing apoptotic cell death, thereby inhibiting lung cancer initiation and progression. Image is created with BioRender.com.

tumorigenesis through genetic and epigenetic reprogramming, our findings support  $\alpha$ -pinene and  $d$ -limonene as promising candidates for lung cancer chemoprevention and therapy. This study demonstrates that the natural terpenes  $\alpha$ -pinene and  $d$ -limonene effectively suppress lung tumor development by blocking the PRC1/ $\beta$ -catenin/GSK-3 $\beta$  signaling pathway and promoting apoptosis. These findings highlight their potential as safe, dietary-based agents for lung cancer chemoprevention and therapy, particularly against carcinogens commonly encountered in the human diet.

#### Ethics approval and consent to participate

All animal experiments followed the guidelines of animal center institute and were approved by the Institutional Animal Care and Use Committee of National Cheng Kung University, Taiwan (Approval No.: 109226).

#### CRedit authorship contribution statement

**Kuo-Ching Huang:** Methodology, Conceptualization, Formal analysis, Writing - Review & Editing.

**Vui-Hyen Chew:** Methodology, Conceptualization, Formal analysis. **Yu-ying Chen:** Methodology, Conceptualization, Formal analysis, Writing - Original Draft, Data Curation. **Huey-Jen Su:** Conceptualization, Supervision. **Hao-Ting Chang:** Methodology, Conceptualization, Formal analysis. **Rong-Jane Chen:** Conceptualization, Writing - Review & Editing, Supervision. **Ying-Jan Wang:** Writing - Review & Editing, Supervision, Funding acquisition, Resources.

#### Funding

This work was supported by the National Science and Technology Council, Taiwan Grants NSTC 113-2314-B-006-067-MY3, NSTC 112-2314-B-006-071.

#### Conflict of interest

The authors declare that they have no known conflict financial interests or personal relationships that could have appeared to influence the work reported in this paper.

## Acknowledgement

We are grateful for the support from the Laboratory Animal Center, Medical college, National Cheng Kung University. The support from the Core Research Laboratory, College of Medicine, National Cheng Kung University. The support from the Instrument Development Center, National Cheng Kung University. Experiments and data analysis were performed in part with the Medical Research Core Facilities Center, Office of Research & Development at China Medical University, Taichung, Taiwan. Graphic abstract image is created with [BioRender.com](https://www.biorender.com).

## References

- [1] Jeon H, Wang S, Song J, Gill H, Cheng H. Update 2025: management of non-small-cell lung cancer. *Lung* 2025;203: 1–15.
- [2] Bray F, Laversanne M, Sung H, Ferlay J, Siegel RL, Soerjomataram I, et al. Global cancer statistics 2022: Globocan estimates of incidence and mortality worldwide for 36 cancers in 185 countries. *CA Cancer J Clin* 2024;74: 229–63.
- [3] Team NLSTR. Reduced lung-cancer mortality with low-dose computed tomographic screening. *N Engl J Med* 2011; 365:395–409.
- [4] Zhang H, Wei H, Han S, Zheng L, Chen X, Li Z, et al. A comprehensive examination of the impact of environmental pollution on lung cancer: a review. *J Adv Res* 2025.
- [5] Casey SC, Vaccari M, Al-Mulla F, Al-Temaimi R, Amedei A, Barcellos-Hoff MH, et al. The effect of environmental chemicals on the tumor microenvironment. *Carcinogenesis* 2015;36:S160–83.
- [6] Kabirai A, Chahar A, Chahar N, Gupta J. Chemical carcinogenesis: a brief review on mechanism & metabolism. *J Oral Med Oral Surg Oral Pathol Oral Radiol* 2020;6:120–4.
- [7] Penny LK, Wallace HM. The challenges for cancer chemoprevention. *Chem Soc Rev* 2015;44:8836–47.
- [8] Menter DG, Bresalier RS. An aspirin a day: new pharmacological developments and cancer chemoprevention. *Annu Rev Pharmacol Toxicol* 2023;63:165–86.
- [9] William Jr WN, Heymach JV, Kim ES, Lippman SM. Molecular targets for cancer chemoprevention. *Nat Rev Drug Discov* 2009;8:213–25.
- [10] Russo GL, Spagnuolo C, Russo M. Reassessing the role of phytochemicals in cancer chemoprevention. *Biochem Pharmacol* 2024;228:116165.
- [11] Ren J, Yan G, Yang L, Kong L, Guan Y, Sun H, et al. Cancer chemoprevention: signaling pathways and strategic approaches. *Signal Transduct Targeted Ther* 2025;10:113.
- [12] Wróblewska-Łuczka P, Cabaj J, Bargiel J, Łuszczki JJ. Anti-cancer effect of terpenes: focus on malignant melanoma. *Pharmacol Rep* 2023;75:1115–25.
- [13] Silva BI, Nascimento EA, Silva CJ, Silva TG, Aguiar JS. Anticancer activity of monoterpenes: a systematic review. *Mol Biol Rep* 2021;48:5775–85.
- [14] Arunasree K. Anti-proliferative effects of carvacrol on a human metastatic breast cancer cell line, MDA-MB 231. *Phytomedicine* 2010;17:581–8.
- [15] Rakoczy K, Szymańska N, Stecko J, Kisiel M, Maruszak M, Niedziela M, et al. Applications of limonene in neoplasms and non-neoplastic diseases. *Int J Mol Sci* 2025;26:6359.
- [16] Zhou Y, Xia J, Xu S, She T, Zhang Y, Sun Y, et al. Experimental mouse models for translational human cancer research. *Front Immunol* 2023;14:1095388.
- [17] Lynch CJ. Studies on the relation between tumor susceptibility and heredity: III. Spontaneous tumors of the lung in mice. *J Exp Med* 1926;43:339–55.
- [18] Chen R-J, Siao S-H, Hsu C-H, Chang C-Y, Chang LW, Wu C-H, et al. TCDD promotes lung tumors via attenuation of apoptosis through activation of the Akt and ERK1/2 signaling pathways. *PLoS One* 2014;9:e99586.
- [19] McGregor DB, Partensky C, Wilbourn J, Rice JM. An IARC evaluation of polychlorinated dibenzo-p-dioxins and polychlorinated dibenzofurans as risk factors in human carcinogenesis. *Environ Health Perspect* 1998;106:755–60.
- [20] Wu C-H, Chen H-L, Su H-J, Lee C-C, Shen K-T, Ho W-L, et al. The topical application of 2, 3, 7, 8-tetrachlorodibenzo-p-dioxin lacks skin tumor-promoting potency but induces hepatic injury and tumor necrosis factor- $\alpha$  expression in ICR male mice. *Food Chem Toxicol* 2004;42:1217–25.
- [21] Malkinson AM, Beer DS. Major effect on susceptibility to urethane-induced pulmonary adenoma by a single gene in BALB/cBy mice. *J Natl Cancer Inst* 1983;70:931–6.
- [22] Sozio F, Schioppa T, Sozzani S, Del Prete A. Urethane-induced lung carcinogenesis. *Methods Cell Biol* 2021;163: 45–57. Elsevier.
- [23] Lajovic A, Nagy LD, Guengerich FP, Bren U. Carcinogenesis of urethane: simulation versus experiment. *Chem Res Toxicol* 2015;28:691–701.
- [24] Parreno V, Martinez A-M, Cavalli G. Mechanisms of polycomb group protein function in cancer. *Cell Res* 2022;32: 231–53.
- [25] Zhan P, Zhang B, Xi G-m, Wu Y, Liu H-b, Liu Y-f, et al. PRC1 contributes to tumorigenesis of lung adenocarcinoma in association with the Wnt/ $\beta$ -catenin signaling pathway. *Mol Cancer* 2017;16:108.
- [26] Chen J, Rajasekaran M, Xia H, Zhang X, Kong SN, Sekar K, et al. The microtubule-associated protein PRC1 promotes early recurrence of hepatocellular carcinoma in association with the Wnt/ $\beta$ -catenin signalling pathway. *Gut* 2016;65:1522–34.
- [27] Chiacchiera F, Rossi A, Jammula S, Piunti A, Scelfo A, Ordóñez-Morán P, et al. Polycomb complex PRC1 preserves intestinal stem cell identity by sustaining Wnt/ $\beta$ -catenin transcriptional activity. *Cell Stem Cell* 2016;18:91–103.
- [28] Qian S, Wei Z, Yang W, Huang J, Yang Y, Wang J. The role of BCL-2 family proteins in regulating apoptosis and cancer therapy. *Front Oncol* 2022;12:985363.
- [29] Chen T, Ashwood LM, Kondrashova O, Strasser A, Kelly G, Sutherland KD. Breathing new insights into the role of mutant p53 in lung cancer. *Oncogene* 2025;44:115–29.
- [30] Odonkor CA, Achilefu S. Differential activity of caspase-3 regulates susceptibility of lung and breast tumor cell lines to Paclitaxel. *Open Biochem J* 2008;2:121.
- [31] Wang Y-J, Chang H, Kuo Y-C, Wang C-K, Siao S-H, Chang LW, et al. Synergism between 2, 3, 7, 8-tetrachlorodibenzo-p-dioxin and 4-(methylnitrosamino)-1-(3-pyridyl)-1-butanone on lung tumor incidence in mice. *J Hazard Mater* 2011;186:869–75.
- [32] Chen R-J, Tsai S-J, Ho C-T, Pan M-H, Ho Y-S, Wu C-H, et al. Chemopreventive effects of pterostilbene on urethane-induced lung carcinogenesis in mice via the inhibition of EGFR-mediated pathways and the induction of apoptosis and autophagy. *J Agric Food Chem* 2012;60:11533–41.
- [33] Gurley KE, Moser RD, Kemp CJ. Induction of lung tumors in mice with urethane. In: *Cold spring harbor protocols* 2015; 2015. p. prot077446.
- [34] Wang B-J, Chen Y-Y, Chang H-H, Chen R-J, Wang Y-J, Lee Y-H. Zinc oxide nanoparticles exacerbate skin epithelial cell damage by upregulating pro-inflammatory cytokines and exosome secretion in M1 macrophages following UVB irradiation-induced skin injury. *Part Fibre Toxicol* 2024;21:9.
- [35] Quintans JS, Shanmugam S, Heimfarth L, Araújo AAS, Almeida JRD, Picot L, et al. Monoterpenes modulating cytokines-A review. *Food Chem Toxicol* 2019;123:233–57.
- [36] Zielińska-Blajet M, Pietrusiak P, Feder-Kubis J. Selected monocyclic monoterpenes and their derivatives as effective anticancer therapeutic agents. *Int J Mol Sci* 2021;22:4763.

- [37] Kumar R, Singh AK, Gupta A, Bishayee A, Pandey AK. Therapeutic potential of Aloe vera—A miracle gift of nature. *Phytomedicine* 2019;60:152996.
- [38] Zhou J, Azrad M, Kong L. Effect of limonene on cancer development in rodent models: a systematic review. *Front Sustain Food Syst* 2021;5:725077.
- [39] Allenspach M, Steuer C.  $\alpha$ -Pinene: a never-ending story. *Phytochemistry* 2021;190:112857.
- [40] Araújo-Filho HGd, Dos Santos JF, Carvalho MT, Picot L, Fruitier-Arnaudin I, Groult H, et al. Anticancer activity of limonene: a systematic review of target signaling pathways. *Phytother Res* 2021;35:4957–70.
- [41] Sanchita, Devi N, Bhattacharya B, Sharma A, Singh I, Kumar P, et al. From citrus to clinic: limonene's journey through preclinical research, clinical trials, and formulation innovations. *Int J Nanomed* 2025;4433–60.
- [42] Castro MA, Rodenak-Kladniew B, Massone A, Polo M, de Bravo MG, Crespo R. Citrus reticulata peel oil inhibits non-small cell lung cancer cell proliferation in culture and implanted in nude mice. *Food Funct* 2018;9:2290–9.
- [43] Galitovskiy V, Chernyavsky AI, Edwards RA, Grando SA. Muscle sarcomas and alopecia in A/J mice chronically treated with nicotine. *Life Sci* 2012;91:1109–12.
- [44] Program NT. NTP toxicology and carcinogenesis studies of d-limonene (CAS No. 5989-27-5) in F344/N rats and B6C3F1 mice (gavage studies). *Natl Toxicol Progr Tech Rep* 1990;347:1–165.
- [45] Kim YW, Kim MJ, Chung BY, Bang DY, Lim SK, Choi SM, et al. Safety evaluation and risk assessment of d-limonene. *J Toxicol Environ Health, Part A B* 2013;16:17–38.
- [46] Adams T, Gavin CL, McGowen M, Waddell W, Cohen SM, Feron V, et al. The FEMA GRAS assessment of aliphatic and aromatic terpene hydrocarbons used as flavor ingredients. *Food Chem Toxicol* 2011;49:2471–94.
- [47] Api A, Belsito D, Botelho D, Bruze M, Burton G, Buschmann J, et al. RIFM fragrance ingredient safety assessment, dL-limonene (racemic), CAS registry number 138-86-3. *Food Chem Toxicol* 2022;161:112764.
- [48] Salehi B, Upadhyay S, Erdogan Orhan I, Kumar Jugran A, LD Jayaweera S, Dias D A, et al. Therapeutic potential of  $\alpha$ - and  $\beta$ -pinene: a miracle gift of nature. *Biomolecules* 2019;9:738.
- [49] Ye Z, Liang Z, Mi Q, Guo Y. Limonene terpenoid obstructs human bladder cancer cell (T24 cell line) growth by inducing cellular apoptosis, caspase activation, G2/M phase cell cycle arrest and stops cancer metastasis. *J BUON* 2020; 25:280–5.
- [50] Hanahan D. Hallmarks of cancer: new dimensions. *Cancer Discov* 2022;12:31–46.
- [51] Mustafa M, Ahmad R, Tantry IQ, Ahmad W, Siddiqui S, Alam M, et al. Apoptosis: a comprehensive overview of signaling pathways, morphological changes, and physiological significance and therapeutic implications. *Cells* 2024; 13:1838.
- [52] Yu X, Lin H, Wang Y, Lv W, Zhang S, Qian Y, et al. D-limonene exhibits antitumor activity by inducing autophagy and apoptosis in lung cancer. *OncoTargets Ther* 2018; 1833–47.
- [53] Zhang Z, Guo S, Liu X, Gao X. Synergistic antitumor effect of  $\alpha$ -pinene and  $\beta$ -pinene with paclitaxel against non-small-cell lung carcinoma (NSCLC). *Drug Res* 2015;65:214–8.
- [54] Qian Z, Li Z, Peng X, Mao Y, Mao X, Li J, et al. Cell death, inflammation, and translational medicine. *J Inflamm Res* 2025;5:655–72.
- [55] Zhu T, Li Q, Xu L, Zhang Q, Lv W, Yu H, et al. Stratification of lung adenocarcinoma patients for d-limonene intervention based on the expression signature genes. *Food Funct* 2021;12:7214–26.
- [56] Tang H, Xiao G, Behrens C, Schiller J, Allen J, Chow C-W, et al. A 12-gene set predicts survival benefits from adjuvant chemotherapy in non–small cell lung cancer patients. *Clin Cancer Res* 2013;19:1577–86.
- [57] Li S, Counter CM. Signaling levels mold the RAS mutation tropism of urethane. *eLife* 2021;10:e67172.
- [58] Li S, MacAlpine DM, Counter CM. Capturing the primordial Kras mutation initiating urethane carcinogenesis. *Nat Commun* 2020;11:1800.